

## Supplementary Materials

### Figure S1

```

human NGF PDB_ID 2IFG 1  SSSHPIFHRGEFSVCD SVSVVWVGDKTTATD IKGKEVMVLGEVNINNSVFKQYFFETKCRD 60
llama NGF PDB_ID 4EFV 1  APSPHPIFHRGEFSVCD SVSVVWVADKTTATD IKGKEVMVLGEVNINNSVFKQYFFETKCRD 60
mouse NGF PDB_ID 1BTG 1  SSTHPVFHMGFEFSVCD SVSVVWVGDKTTATD IKGKEVTVLAEVNINNSVFRQYFFETKCRA 60
: . : ** : ** ***** , ***** ** , ***** : *****

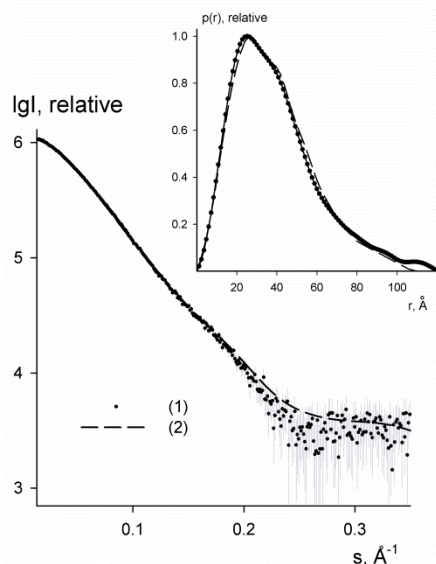
human NGF PDB_ID 2IFG 61  PNPVDSGCRGIDSKHWNSYCTTHTFVKALTMDGKQAAWRFIRIDTACVCLSRKAVRRA 120
llama NGF PDB_ID 4EFV 61  PNPVASGCRGIDSKHWNSYCTTHTFVKALTMDGKQAAWRFIRIDTACVCLSKKAS --- 117
mouse NGF PDB_ID 1BTG 61  SNPVESGCRGIDSKHWNSYCTTHTFVKALTTDEKQAAWRFIRIDTACVCLSRKATRRG 120
. *** ***** * ***** : **

```

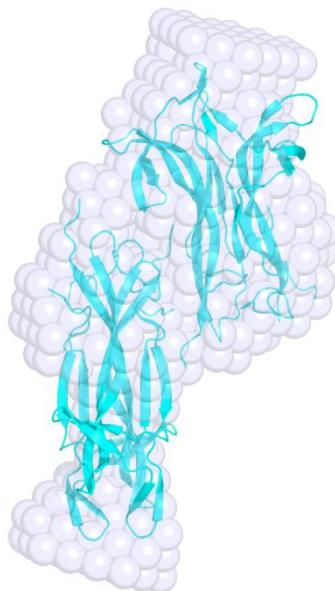
**Figure S1. Multiple sequence alignment of hNGF with the templates employed to build a complete model.** The missing residues in the starting model of hNGF (PDB\_ID 2IFG) that have been built are underlined.

### Figure S2

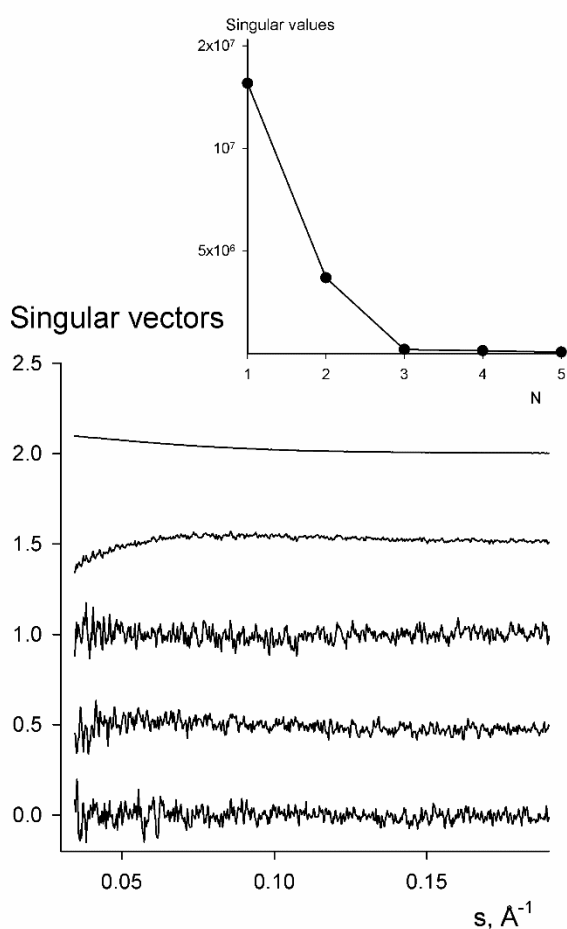
**A**



**B**



**Figure S2. Preliminary SAXS studies of the hNGF.** (A) Experimental X-ray solution scattering pattern of the hNGF at the concentration of 5.5 mg/mL (dots with error bars). The theoretical solution scattering curve was computed with CRY SOL (1) using as a model a mNGF DD molecular assembly extracted from the observed crystal structure (PDB\_ID 1BTG) (2) (dashed line). All the plots display the logarithm of the scattering intensity  $I$  as a function of momentum transfer  $s = [4\pi\sin(\theta/2)] / \lambda$  ( $\text{\AA}^{-1}$ ) where  $\theta$  is the scattering angle and  $\lambda = 1.5 \text{ \AA}$  is the X-ray wavelength. The distance distribution function calculated from the experimental data is displayed in the insert of the plots (solid lines), the  $p(r)$  from the crystallographic model of the mNGF DD is shown with dashed line. (B) *Ab initio* shape determination of hNGF from the scattering data: cartoon representation of the crystallographic DD assembly of mNGF, PDB\_ID 1BTG (2), superimposed on the model (light blu spheres), obtained *ab initio* by DAMMIN (3). Figure created by the program *Pymol* (4).

**Figure S3**

**Figure S3. Singular value decomposition of SAXS data on hNGF.** Only two significant singular values (shown in the insert) corresponding to two non-randomly oscillating singular vectors were found. It suggests that the system can be described by two independent components thus validating our choice of two oligomeric species (dimers and DD) for SAXS data modelling.

**Table S1: Distribution (%) of the hNGF dimers and dimers of dimers molecular assemblies in solution, as assessed by SAXS concentration dependent experiments**

Concentration (mg/mL)	$\chi$	$R_g(\text{Exp}) \text{ \AA}$	% dimer <sup>(a)</sup>	% dimer of dimers <sup>(b)</sup>
0.43	1.23	20.7±0.5	100	0
1.98	1.16	21.7±0.5	82±5	18±5
2.75	1.32	24.0±0.5	56±5	44±5
3.77	1.36	24.8±0.5	49±5	51±5
5.5	1.95	29.0±0.5	7±5	93±5

<sup>[a]</sup>  $R_g(\text{Calc}) = 21.0 \text{ \AA}$  based on the reconstructed model of the hNGF dimer

<sup>[b]</sup>  $R_g(\text{Calc}) = 28.5 \text{ \AA}$  based on the selected hNGF dimer of dimer docking solution

## Supplementary References

1. Svergun, D.I., Barberato, C., and Koch, M.H.J. 1995. CRY SOL - a Program to Evaluate X-ray Solution Scattering of Biological Macromolecules from Atomic Coordinates. *J. Appl. Crystallogr.* 28:768-773.
2. Holland, D.R., Cousens, L.S., ..., Matthews, B.W. 1994. Nerve growth factor in different crystal forms displays structural flexibility and reveals zinc binding sites. *J. Mol. Biol.* 239:385-400.
3. Svergun, D.I. 1999. Restoring low resolution structure of biological macromolecules from solution scattering using simulated annealing. *Biophys. J.* 76:2879-2886.
4. DeLano, W.L. 2002. The PyMOL Molecular Graphics System. DeLano Scientific LLC, Palo Alto, CA, USA. <http://www.pymol.org>.